

# Modeling femtosecond pulse propagation and high harmonics generation in hollow core fibers

Valer Tosa<sup>1,\*</sup>, Anna Gabriella Ciriolo<sup>2</sup>, Rebeca Martinez Vazquez<sup>2</sup>, Caterina Vozzi<sup>2</sup>, and Salvatore Stagira<sup>3</sup>

<sup>1</sup>National Institute for R&D Isotopic and Molecular Technologies, 400293 Cluj Napoca, Romania

<sup>2</sup>Institute for Photonics and Nanotechnologies (IFN), National Research Council (CNR), Milano, Italy

<sup>3</sup>Politecnico di Milano, Physics Department, Milano, Italy

**Abstract.** One way to increase the well known low efficiency of high order harmonics generation is to place the gas medium in a hollow core waveguide. The numerical model used to obtain driving and harmonics field configuration along and across the waveguide was developed for an arbitrary gas density profile and arbitrary fiber diameter modulation. The model was tested against experimental measurements and excellent agreement was obtained for the fluorescence emission along the waveguide. We analyse the influence of the diameter modulation which result from the fabrication process on both pulse propagation and on harmonic generation.

## 1 Introduction and methods

High order harmonic generation (HHG) in gas, despite the low efficiency of the process, remains one of the main methods to obtain extreme ultra-violet (XUV) or soft X-ray attosecond pulses. Using guided structures to propagate the ultrafast pulse is one way to increase the HHG yield and thus is of great practical interest. Indeed, capillaries allow achieving both laser beam and gas confinement for a longer interaction length, thus leading to a significant increase of the generation yield. Moreover, capillaries can be filled with gas both in static and continuous-flow regimes, so that they can be used in combination with high-repetition-rate laser systems.

The integrated microfluidic glass device devoted to XUV generation by HHG in gas medium is composed [1] of a main micro-channel that works as a hollow-core waveguide (HCW) for the propagation of the femtosecond laser pulse. The interaction region is filled with the working gas using a micro-structured network of delivery channels fabricated in the same glass substrate. High-order harmonics of the fundamental field are generated within the waveguide by the well-known three step process happening in every optical cycle of the laser field: ionization, acceleration and recombination of the electron found in the outermost shell of the atom.

While the elementary three step process is well understood and described at quantum level, the macroscopic build up of the signal from the single radiating dipoles in the interaction volume is difficult to control experimentally and not easy to describe phenomenologically as it depends on many intensive and extensive parameters.

When building a model for HHG in macroscopic media [2] a first necessary step is solving the driving

field propagation in the ionizing gas. We solved this problem by starting from the wave equation in time domain, then transforming it in the moving frame and in frequency domain. We then used the split-step method for advancing each spectral component along the propagation direction while assuming the field as a superposition of  $EH_{11}$  eigenmodes [3] to satisfy the boundary conditions in the hollow dielectric waveguide.

The second step is to estimate the response of the atom to the propagated field and this was calculated in the SFA approximation [4]. The time-dependent resulting polarization was eventually used as a source term in the wave equation for the harmonic field which was solved in a similar way as for the driving field. The far field was obtained taking into account the experimental configuration by solving the Hankel transform for spectral components of the harmonic field.

Our model allows for an arbitrary density distribution of the gas along the propagation direction. The density distribution was obtained in a separate investigation by solving the gas flow problem in the specific topology of the fabricated structure.

## 2 Testing the pulse propagation model

Solving the problem of pulse propagation in a HCW is the first essential step in modeling HHG. The method we used for the case of free space propagation [2,5] was adapted for fiber case as briefly described in the preceding section.

The numerical model takes into account a refractive index which is space-time dependent having contributions of dispersion from fiber and neutrals, as well as nonlinear contributions from Kerr and ionization effects. We note here that for all HHG experiments

\* Corresponding author: [tosa@itim-cj.ro](mailto:tosa@itim-cj.ro)

ionization is the necessary ingredient and it induces the dominant term in the refractive index build-up. The contribution of the nonlinear terms to pulse propagation was included in the second step of split step method.

Testing the model against experimental data was a necessary step in the model development. In the following we present simulation results of the model for conditions closed to a specific experimental situation [6]. In particular we consider a 5 cm long capillary with a 75  $\mu\text{m}$  radius hole filled with argon at a pressure of 80 mbar in the central part of the capillary; the Ar pressure increases over 3 mm from 0 to 80 mbar at the fiber input. Laser pulses of 0.5 mJ energy, and 40 fs duration at 800 nm wavelength are focused with a 40 cm focal length element producing a Gaussian waist of 48  $\mu\text{m}$  and an initial peak intensity of  $3.8 \times 10^{14} \text{ W/cm}^2$ .

In the experiment [6] the plasma emission from the ionized Ar was recorded from the side of the waveguide as function of the propagation coordinate  $z$  (see for example Fig. 9 of [6]).

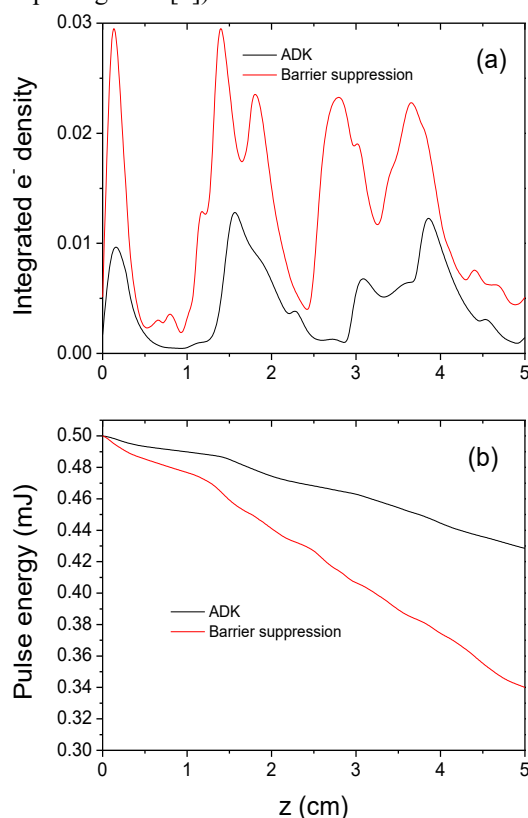


Fig.1 Total electron density (a) and pulse energy (b) as a function of  $z$  position along the HCW, for two ionization models, as detailed in the text.

In the modeling we calculated the total density of electrons (integrated across HCW area) and plotted it along the  $z$  coordinate, as seen in Fig. 1.a. The pulse energy is also shown in Fig. 1.b for the same conditions. The calculations have been done using two different models for the calculation of the Ar ionization rates: the classical ADK rates [7] and the static field ionization rates in the barrier-suppression regime [8]. The later yields ionization rates higher by almost one order of magnitude in the  $10^{14} \text{ W/cm}^2$  range of intensities. This difference is reflected in both the integrated electron

density and the pulse energy, higher ionization rates producing the obvious increase of the total electron yield but also the splitting of the density profile. Higher ionization rates also induce a larger pulse energy loss which is consumed for atoms ionization. The comparison with experimental data favors the ADK rates which yield a closer agreement to the experiment both on plasma profile and on pulse energy dependence on propagation distance.

We also show in Fig. 2 the evolution of the energies contained in the first three modes, to demonstrate that almost 90% of the energy is initially in the fundamental mode.

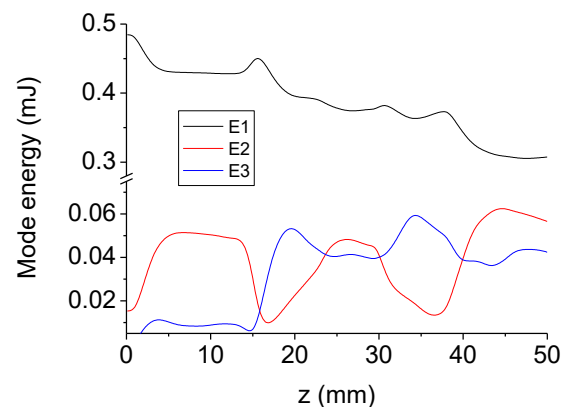


Fig.2 The energies contained in the first three modes

### 3 Laser pulse propagation in straight and modulated HCW

After the fabrication process [9] the hollow waveguide surface presents a ripple pattern, with a periodicity of about 5  $\mu\text{m}$ , made of parallel grooves perpendicular to laser scanning direction. As the surface quality of the HCW walls influences the propagation of pulsed radiation, we here investigate the behaviour, in terms of driving field propagation and harmonics yield, between two devices characterized by the same internal structure, one with the typical surface roughness as resulting from the etching process and one smoothed by a thermal process.

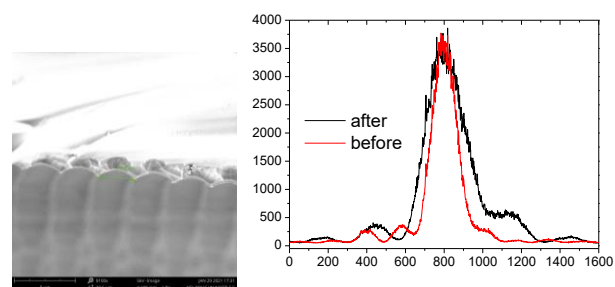


Fig. 3 Left: HCW profile along the channel, showing ripples of about 5  $\mu\text{m}$  period. Right: Beam profile at fiber exit before and after thermal treatment, arbitrary units on both axes.

The experimental measurement of the beam profile at HCW exit shows clearly that the ripple pattern influences the pulse propagation. Shown in Fig. 3 is the radial profile of the beam at exit before and after thermal treatment which reduces the deepness of the modulation.

The width of the beam is larger after thermal treatment which suggests better conditions for propagation.

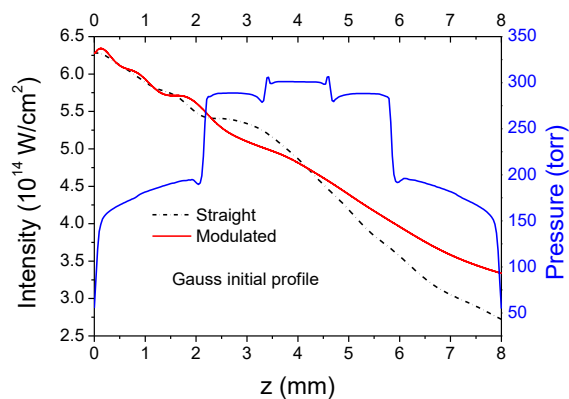


Fig. 4 On-axis peak intensity along the channel for the straight and a modulated HCW. The density profile of the He gas is also shown.

The modeling followed closely the experimental conditions: a pulse of 25 fs duration and 0.45 mJ energy propagates along a HCW of 140  $\mu\text{m}$  diameter and 8 mm long, filled with He having a profile of density as shown in Fig. 4 (blue solid line). The on-axis peak intensity of the pulse along the channel is shown for both modulated (red solid line) and straight channel (black dash dot line). The initial radial beam profile was set to Gaussian with an optimized waist for coupling into the waveguide.

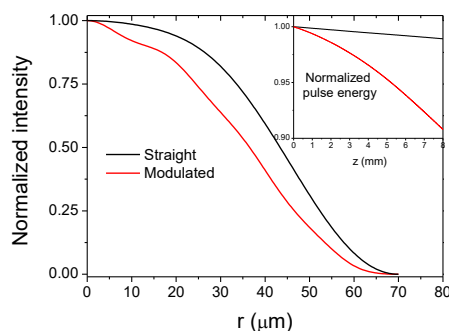


Fig. 5 Beam radial profile at HCW exit for the straight (black) and modulated (red) channel. The inset shows the evolution of the pulse energy along propagation direction.

The radial field profile at HCW exit is shown in Fig. 5 for the two cases. The straight case yields a larger waist (57.3  $\mu\text{m}$  at  $1/e^2$ ) than the modulated case (52.6  $\mu\text{m}$  at  $1/e^2$ ), in very good agreement with the experimental findings. The evolution of the pulse energy (shown in the inset of Fig. 5) confirms that the ripples enhance the losses in the channel during propagation.

#### 4 Harmonic generation in straight and modulated HCW

As known, intensity variation of the driving field will induce phase variations for the induced dipole which is the source for the harmonic field. With this picture in mind we simulated the generation of harmonics in the two considered cases.

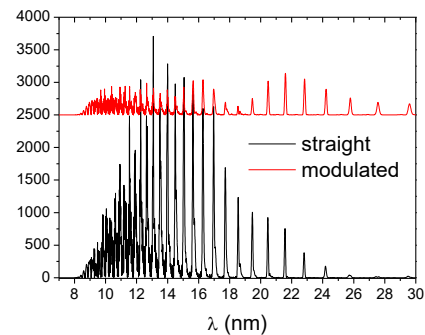


Fig. 6 Far field power spectra for the straight (black) and modulated (red) fiber. For better visibility the later is shifted on vertical axis, but (arbitrary) units are the same.

Shown in Fig. 6 is the far field power spectra for the straight (black line) and for the modulated HCW, the latter is shifted on vertical axis to see better the differences between them. As clearly seen, the modulated spectrum is about an order of magnitude weaker than the straight fiber spectrum. Also, from the analysis of the far field profiles of the harmonics (not shown here) we conclude that they are emitted with a larger angle in the modulated fiber case.

In conclusion we investigated femtosecond pulse propagation and harmonic generation in HCW both in ideal conditions of surface quality and in modulated channel diameter caused by the fabrication process. Both fields are affected by the propagation, especially the harmonic field which suffer from the local variations of the intensity.

Acknowledgements: Funding from the European Union's Horizon 2020 research and innovation programme under grant agreement No 964588, and MIUR PRIN "aSTAR" 2017RKWTMY.

#### References

1. A. G. Ciriolo et al., *J. Phys - Photonics* **2**, 024005 (2020)
2. V. Tosa, H.T. Kim, I.J. Kim, and C.H. Nam *Phys. Rev. A* **71**, 063807 (2005)
3. E.A.J. Marcatili, R.A. Schmelzter *The Bell System Technical Journal* **43**, 1783 (1964)
4. M. Lewenstein, Ph. Balcou, M.Y. Ivanov, A. L'Huillier, P. B. Corkum, *Phys. Rev. A.* **49** 2117 (1994)
5. V. Tosa, K. Kovacs, B. Major, E. Balogh, K. Varju, *Quant. Electronics* **46** 321(2016)
6. C.A. Froud, R.T Chapman, E.T.F. Rogers, M. Praeger, B Mills, J. Grant-Jacob, T.J. Butcher, S.L. Stebbings, A.M. de Paula, J.G. Frey, and W.S. Brocklesby . *J. Opt. A* **11**, 054011 (2009)
7. V.S Popov, *Physics Uspekhi* **47**, 855 (2004)
8. X.M. Tong and C.D. Lin, *J. Phys. B: At. Mol. Opt. Phys.* **38**, 2593 (2005)
9. R. Martinez Vazquez, A. G. Ciriollo, G. Crippa, V. Tosa, F. Salla, M. Devetta, C. Vozzi, S. Stagira, R. Osellame, *International Journal of Applied Glass Science*, accepted 2021